

# Extended averaging technique for derivation of error-compensating algorithms in phase-shifting interferometry

Joanna Schmit and Katherine Creath

Phase-shifting interferometry suffers from two main sources of error: phase-shift miscalibration and detector nonlinearity. Algorithms that calculate the phase of a measured wave front require a high degree of tolerance for these error sources. An extended method for deriving such error-compensating algorithms patterned on the sequential application of the averaging technique is proposed here. Two classes of algorithms were derived. One class is based on the popular three-frame technique, and the other class is based on the 4-frame technique. The derivation of algorithms in these classes was calculated for algorithms with up to six frames. The new 5-frame algorithm and two new 6-frame algorithms have smaller phase errors caused by phase-shifter miscalibration than any of the common 3-, 4- or 5-frame algorithms. An analysis of the errors resulting from algorithms in both classes is provided by computer simulation and by an investigation of the spectra of sampling functions.

*Key words:* Interferometry, optical testing.

## 1. Introduction

In interferometry the phase-shifting technique is well known as a method for retrieving a wave-front phase encoded in the interference fringes. This technique requires the registration of a few frames of fringes by means of CCD camera. The interfering reference wave front is sequentially shifted in phase from frame to frame with respect to the measured wave front. This method of phase measurement has been applied to many areas of precision metrology, where the phase shift can be realized in a number of ways.<sup>1,2</sup> The conventional phase-shifting technique is based on the synchronous detection method,<sup>3</sup> in which the phase of the incoming sinusoidal signal is measured. The sinusoidal signal is sampled and correlated with sinusoidal and cosinusoidal reference signals. In interferometry the intensity of the incoming signal to each pixel is modulated in the sinusoidal fashion as the reference wave front is being shifted. The phase

of the signal can then be calculated according to

$$\tan \varphi = \frac{\sum_{m=1}^M I_m \sin[2\pi(m-1)/M]}{\sum_{m=1}^M I_m \cos[2\pi(m-1)/M]}, \quad (1)$$

where  $I_m = I(x, y)[1 + \gamma(x, y)\cos[\varphi(x, y) + 2\pi(m-1)/M]]$  is the intensity distribution in the sampled  $m$ th frame,  $\varphi(x, y)$  is a measured wave front (phase),  $\gamma(x, y)$  is the fringe contrast, and  $2\pi/M$  is a temporal phase shift. For four acquired frames the phase shift equals  $\pi/2$ , simplifying the equation to

$$\tan \varphi = -\frac{I_2 - I_4}{I_1 - I_3}, \quad (2)$$

which is the algorithm for the conventional four-frame method.<sup>4</sup>

Other simple phase-shifting algorithms exist; however, they result in relatively large phase errors.<sup>2</sup> Some of those algorithms are based on analytical solutions,<sup>5</sup> and others are based on the least-squares technique,<sup>6,7</sup> which is a more general phase-calculating method that utilizes a synchronous detection technique. In an attempt to reduce phase error, researchers developed families of error-compensating algorithms with  $M + 1$  samples over one full period of

The authors are with the Optical Sciences Center, University of Arizona, Tucson, Arizona 85721.

Received 3 May 1994; revised manuscript received 27 September 1994.

0003-6935/95/193610-10\$06.00/0.

© 1995 Optical Society of America.

signal<sup>8,9</sup>; the most common of these was the five-frame algorithm.<sup>10</sup> While still requiring a relatively low number of grabbed frames, this algorithm produces the smallest error resulting from phase-shift miscalibration and is insensitive to detector nonlinearity. A different approach to the derivation of error-compensating algorithms, called the averaging technique, was proposed by Schwider *et al.*<sup>11</sup> in 1983. Our paper extends this method for deriving algorithms.

A new error-compensating algorithm can be calculated from an existing algorithm if two sets of data with a  $\pi/2$  shift in the initial phase are taken. This process may require the acquisition of twice as many frames and may result in a complicated algorithm. However, if the averaging technique is applied to algorithms that require a  $\pi/2$  phase shift between frames, then only one more frame is needed and a simple algorithm can be derived. Recently Schwider *et al.*<sup>12</sup> derived a new 4-frame error-compensating algorithm with a  $\pi/2$  phase shift that produced smaller errors than the conventional 4-frame method. This paper demonstrates that the averaging technique procedure can be applied sequentially and that each new algorithm yields smaller errors than the algorithm from which it was derived. Two classes, A and B, of error-compensating algorithms were calculated by use of this procedure. Class A is based on the 3-frame method and class B is based on the 4-frame method. In each class, algorithms requiring up to six frames were derived (grouped in Subsection 3.B), but further extensions to seven frames (and so on) are possible.

We provide a sequential discussion of both classes of algorithms, starting with a review of the basic algorithms (Subsections 2.B and 2.C) and continuing to our discussion of the new 5- and 6-frame algorithms. The 5-frame algorithm from class A and the 6-frame algorithms from class A and B have not yet been presented in the literature and are derived in Section 3. These new error-compensating algorithms are less sensitive to phase-shift miscalibration than any of the existing algorithms while still requiring a reasonably small number of collected frames. We demonstrate the effectiveness of these new algorithms in Subsections 4.A and 4.B by comparing the phase errors caused by phase-shift miscalibration and second-order detector nonlinearity with errors in the previously known 4- and 5-frame algorithms. The error analysis presented here is done in two ways. The first analysis is based on computer simulation rather than a theoretical derivation of the residual error, because the computer simulation permits a closer approximation of actual conditions. The second analysis investigates the spectra of the sampling functions to judge the sensitivity of the algorithms to different error sources; this is explained in detail in Subsection 4.C.

## 2. Background of the Averaging Technique

The basic source of errors in phase-shifting interferometry is phase-shift miscalibration. The resulting

phase error is proportional to  $\cos 2\phi$  and  $\sin 2\phi$  of the measured phase,  $\phi$ . This error has been well examined, in theory, through experimentation and by computer simulation.<sup>1,2</sup> In phase-shifting techniques this type of error can be a problem because the fringes are usually nulled out, resulting in a phase error with a large period. The fringes are nulled out to avoid errors caused by the different traveling paths of the reference and measured wave fronts. This error is difficult to remove by filtering (e.g., by  $3 \times 3$  pixel filtering) because its period is usually greater than the size of the filter window; thus this error becomes part of the measured wave front. To reduce this error, one takes two data sets with a  $\pi/2$  initial phase shift and averages the resulting two phase maps.<sup>13</sup> Schwider proposed that instead of calculating the phase map twice and then averaging, one could merge the two data sets together into a phase calculation of the following form<sup>11</sup>:

$$\tan \phi = \frac{N_1 + N_2}{D_1 + D_2}, \quad (3)$$

where  $N_i$  and  $D_i$  are the numerator and denominator of Eq. (1) for each set of data. This is called the averaging technique.

### A. Extended Averaging Technique

The averaging technique, when applied to two sets of  $M$  frames shifted by  $\pi/2$  in the initial phase, does not completely eliminate the twice-the-fringe-frequency phase error as it follows from Schwider first-order approximation,<sup>11</sup> but it does significantly reduce this error. We demonstrate this in Section 4. The error-compensating algorithm for  $2M$  frames can be calculated, although the resulting algorithm may be complicated because of the amount of data required. However, we can reduce the acquisition and processing time if the phase shift between the frames equals  $\pi/2$ . In this case only one additional frame is needed because the first data set overlaps with the second, resulting in a fairly simple  $M + 1$  frame algorithm. This procedure can be reapplied successively to two sets of  $M + 1$  frames; we then obtain an  $M + 2$  algorithm with an even smaller twice-the-fringe-frequency error. By applying the averaging technique twice in sequential fashion to data with  $\pi/2$  phase shifts between frames, we require only  $M + 2$  frames instead of  $3M$  frames and the phase error is reduced with each procedure. The sequential derivations of the new error-compensating algorithms may be represented in the following forms. For the  $M$ -frame algorithm we have

$$\tan \phi_M = \frac{N}{D}, \quad (4a)$$

which is the basic equation for successive algorithms in this extended averaging technique.

The  $M + 1$ -frame algorithm according to the

averaging technique can be written as

$$\tan \varphi_{M+1} = \frac{N_1 + N_2}{D_1 + D_2} = \frac{N'}{D'}. \quad (4b)$$

Applying the averaging technique again we obtain the  $M + 2$ -frame algorithm:

$$\tan \varphi_{M+2} = \frac{N' + N''}{D' + D''} = \frac{N_1 + 2N_2 + N_3}{D_1 + 2D_2 + D_3}, \quad (4c)$$

where  $N_{1,2,3}$  and  $D_{1,2,3}$  are the numerators and denominators for first, second, and third runs of  $M$  data sets, respectively, and  $N', D'$  are those of first and second  $M + 1$  data sets. The equations for a greater number of frames follow from this procedure.

In the calculation of error-compensating algorithms the choice of the basic equation is arbitrary, but for the best results the equation with the smallest number of frames and the smallest phase error should be chosen. In this paper the well-known 3- and 4-frame algorithms with  $\pi/2$  phase shift are chosen as basic equations. By applying this technique sequentially, one can derive the algorithm for any number of frames. The degree of tolerance for the phase error and the number of frames collected depends on the user's requirements. Note that the signal does not have to be sampled over its period (as in most algorithms) but rather over the multiple of  $\pi/2$ .

#### B. 5A-Frame Error-Compensating Algorithm Derived from the 4A-Frame Algorithm

Schwider *et al.*<sup>11</sup> employed their averaging technique to the conventional 4-frame method for two data sets,

$$-\frac{I_2 - I_4}{I_1 - I_3} = \frac{N_1}{D_1}, \quad (5a)$$

$$-\frac{I_2 - I_4}{I_5 - I_3} = \frac{N_2}{D_2}, \quad (5b)$$

and derived a 5-frame error-compensating algorithm by substituting Eqs. (5) into Eq. (3):

$$\tan \varphi = -\frac{2(I_2 - I_4)}{I_1 + I_5 - 2I_3}. \quad (6)$$

The effectiveness of this method has been studied by several authors.<sup>8-11,14</sup> In examining the residual phase error caused by linear phase-shift miscalibration in this method, Schwider *et al.*<sup>11</sup> used first-order approximations for  $\sin(\varepsilon)$  and  $\cos(\varepsilon)$ , where  $\varepsilon$  is phase-shift miscalibration, and found that the residual error is only a constant offset and of no interest in measurement. The 5-frame method was revised and more fully analyzed by Hariharan *et al.*<sup>10</sup> In addition, Surrel<sup>9</sup> presented a more general approach for calculating the residual error for phase-shifting methods. Both authors used second-order approximations for sine and cosine functions and found that the peak-to-valley (P-V) residual error is proportional to the

square of the linear phase-shift miscalibration and that the dependence on phase is proportional to  $\sin 2\varphi$ . These results agree with the computer-simulated errors obtained by Creath.<sup>14</sup> The P-V error in the 5-frame technique is significantly smaller than in the conventional 4-frame technique; however, the double-frequency character of the phase error remains. This error-compensating method has become very popular in phase-measuring interferometric systems because of its tolerance for phase-shift miscalibration. This 4-frame algorithm is the basic equation for algorithms in class A and is called the 4A-frame algorithm. The popular 5-frame algorithm will be called here the 5A-frame algorithm.

#### C. 4B-Frame Error-Compensating Algorithm Derived from the 3B-Frame Algorithm

Recently Schwider *et al.*<sup>12</sup> reemployed the averaging technique in deriving a 4-frame error-compensating algorithm from the 3-frame method with  $\pi/2$  phase steps between frames. This 3-frame algorithm is the basic equation for algorithms in class B. We call this the 3B-frame algorithm. For the first set of data the equation is

$$-\frac{-I_1 + 2I_2 - I_3}{I_1 - I_3} = \frac{N_1}{D_1}, \quad (7a)$$

and for the second data set with  $\pi/2$  offset it is

$$-\frac{I_2 - I_4}{I_2 - 2I_3 + I_4} = \frac{N_2}{D_2}. \quad (7b)$$

As a result an algorithm for a new four-frame method, which we call the 4B-frame algorithm, was derived:

$$\tan \varphi = -\frac{-I_1 + 3I_2 - I_3 - I_4}{I_1 - 3I_3 + I_2 + I_4}. \quad (8a)$$

The simpler form of this algorithm is

$$\tan \left( \varphi + \frac{\pi}{4} \right) = -\frac{2(I_2 - I_3)}{I_1 - I_2 - I_3 + I_4}. \quad (8b)$$

The experimental results presented in the paper by Schwider *et al.*<sup>12</sup> showed that this algorithm yielded smaller errors than the conventional 4-frame algorithm. In calculating the residual phase error caused by phase-shift miscalibration, the authors again used only first-order approximations, which resulted in a constant offset in phase.

### 3. New Error-Compensating Algorithms

#### A. New 5B-Frame Error-Compensating Algorithm Derived from the 4B-Frame Algorithm

All of the developed error-compensating algorithms presented in the previous subsection show much smaller errors than the algorithms from which they were derived. Employing our extended averaging technique to the 4B-frame algorithm, we obtained a new 5B-frame algorithm. The two equations for two

sets of four-frame data with an initial  $\pi/2$  phase shift are in the form

$$-\frac{-I_1 + 3I_2 - I_3 - I_4}{I_1 - 3I_3 + I_2 + I_4} = \frac{N_1}{D_1}, \quad (9a)$$

$$-\frac{I_2 + I_3 - 3I_4 + I_5}{I_2 - 3I_3 + I_4 + I_5} = \frac{N_2}{D_2}. \quad (9b)$$

Using Eqs. (9a) and (9b) in Eq. (3), we find that the new algorithm is

$$\tan \varphi = -\frac{-I_1 + 4I_2 - 4I_4 + I_5}{I_1 + 2I_2 - 6I_3 + 2I_4 + I_5}. \quad (10a)$$

This can be simplified to

$$\tan\left(\varphi + \frac{\pi}{4}\right) = -\frac{3I_2 - 3I_3 - I_4 + I_5}{I_1 - I_2 - 3I_3 + 3I_4}. \quad (10b)$$

#### B. Two Classes of Algorithms

We chose two basic equations, Eqs. (5a) and (7a), to derive our error-compensating algorithms by using the extended averaging technique. We carried our derivations up to algorithms that employ six frames of collected data. These are grouped in Table 1. Algorithms in class A are based on the 3-frame method; algorithms in class B are based on the 4-frame method. Each of the algorithms is presented in two forms: the first for zero phase offset in the reference signal, and the second with offset  $\pi/4$ . Essentially both forms result in the same errors from the sources considered here, as the resulting phase differs only by a constant offset in the whole measured wave front. The algorithms from class A for  $M$  frames are referred to as *MA*-frame algorithms, and those from class B are referred to as *MB*-frame algorithms.

#### 4. Error Comparison in Algorithms from Classes A and B

Here we compare the phase errors in the algorithms for four, five, and six frames from both classes, specifically examining the linear phase-shift miscalibration and second-order detector nonlinearity. The phase errors and their P-V errors are presented

in the form of plots. Our analysis was done on computer-generated interferograms with  $128 \times 128$  pixel resolution and 8-bit intensity resolution.

##### A. Linear Phase-Shift Miscalibration

The actual phase shift between frames can be expressed as

$$\alpha = \frac{\pi}{2}(1 + \delta), \quad (11)$$

where  $\pi/2$  is the required phase shift and  $\delta$  is a normalized phase-shift miscalibration. The intensity in the  $m$ th interferogram is then

$$I_m^{(x,y)} = I(x,y) \left[ 1 + \gamma(x,y) \cos \left[ \frac{m\pi}{2}(1 + \delta) \right] \right]. \quad (12)$$

For our analysis of the characteristics of phase error, we generated five interferograms with three fringes. No noise was added for better observation of the twice-the-frequency phase error. The phase-shift miscalibration was chosen to equal 20%. The phase error was calculated for each algorithm from a single set of interferograms. Results are presented in Fig. 1. The basic 4A-frame method results in a large phase error at double the fringe frequency caused by phase-shift miscalibrations. The phase error in the 4B-frame and the 5A-frame algorithms is much smaller and of the same amplitude in both methods. For the 5B-frame and 6A-frame algorithms the double-fringe frequency error is even smaller but still noticeable. The 6B-frame algorithm shows the smallest error; its value is insignificant for most of the measurements.

To show the differing sensitivities of each of the algorithms to phase-shift miscalibration, we diagrammed the P-V phase error versus the phase-shift error, shown in Fig. 2. The interferograms were generated without noise, so the P-V values are pure errors caused by phase-shift error only. From the P-V phase error plot we can see that the 4B-frame algorithm results in the same error as the 5A-frame technique. The only difference is that the number of collected frames has been reduced from five to four.

Table 1. Algorithms in Classes A and B

Frame No.	Class A		Class B	
	$-\tan(\varphi)$	$-\tan(\varphi + \pi/4)$	$-\tan(\varphi)$	$-\tan(\varphi + \pi/4)$
Three			$\frac{-I_1 + 2I_2 - I_3}{I_1 - I_3}$	$\frac{I_2 - I_3}{-I_2 + I_1}$
Four	$\frac{I_2 - I_4}{I_1 - I_3}$	$\frac{I_1 + I_2 - I_3 - I_4}{I_1 - I_2 - I_3 + I_4}$	$\frac{-I_1 + 3I_2 - I_3 - I_4}{I_1 - 3I_3 + I_2 + I_4}$	$\frac{2(I_2 - I_3)}{I_1 - I_2 - I_3 + I_4}$
Five	$\frac{2I_2 - 2I_4}{I_1 - 2I_3 + I_5}$	$\frac{I_1 + 2I_2 - 2I_3 - 2I_4 + I_5}{I_1 - 2I_2 - 2I_3 + 2I_4 + I_5}$	$\frac{-I_1 + 4I_2 - 4I_4 + I_5}{I_1 + 2I_2 - 6I_3 + 2I_4 + I_5}$	$\frac{3I_2 - 3I_3 - I_4 + I_5}{I_1 - I_2 - 3I_3 + 3I_4}$
Six	$\frac{3I_2 - 4I_4 + I_6}{I_1 - 4I_3 + 3I_5}$	$\frac{I_1 + 3I_2 - 4I_3 - 4I_4 + 3I_5 + I_6}{I_1 - 3I_2 - 4I_3 + 4I_4 + 3I_5 - I_6}$	$\frac{-I_1 + 5I_2 + 2I_3 - 10I_4 + 3I_5 + I_6}{I_1 + 3I_2 - 10I_3 + 2I_4 + 5I_5 - I_6}$	$\frac{4(I_2 - I_3 - I_4 + I_5)}{I_1 - I_2 - 6I_3 + 6I_4 + I_5 - I_6}$

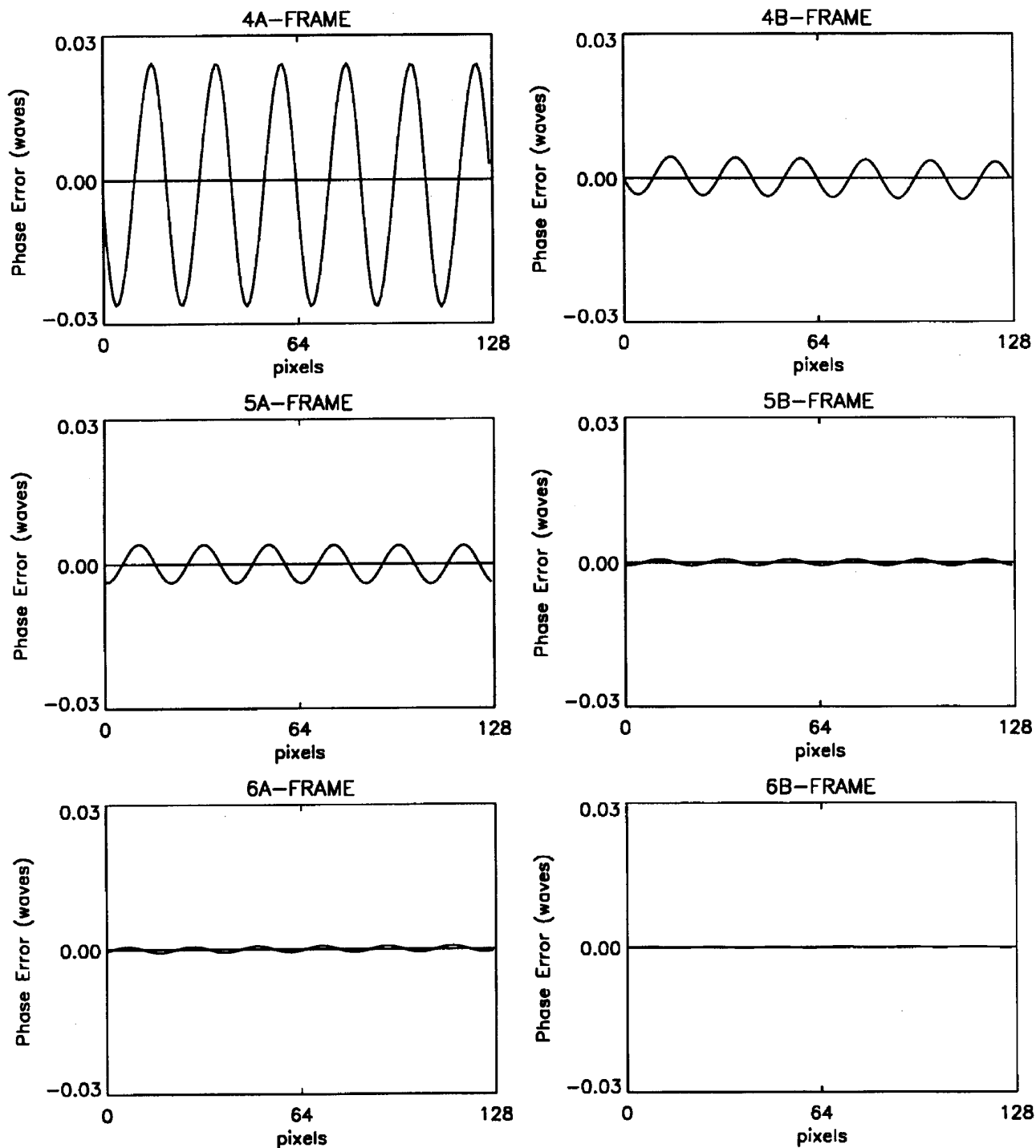


Fig. 1. Phase error for three intensity fringes caused by 20% phase-shift miscalibration.

From this same plot, moreover, we can see that the 5B-frame technique yields the same error as the 6A-frame technique, requiring one less frame. The 6B-frame technique is the least sensitive to phase-shift errors of any of the methods considered. The algorithm's tolerance for phase-shift miscalibration is especially important for measurements of wave fronts in a converging beam, where the phase shift at the center is different from that at the edges of the beam.<sup>15</sup>

#### B. Second-Order Detector Nonlinearity

The response of the detector to the incident intensity can be nonlinear, with the most common nonlinearity being of the second order. The detected  $I'$  intensity is then

$$I'(x, y) = I(x, y) + \delta I^2(x, y), \quad (13)$$

where  $I$  is the incident intensity and  $\delta$  is a normalized error in the detected intensity.

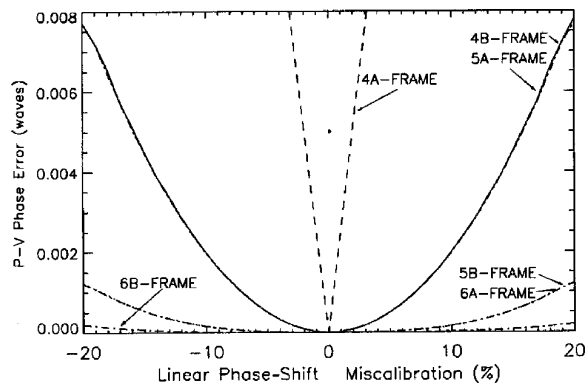


Fig. 2. P-V phase error versus percent of phase-shift miscalibration.

The algorithms of class A are not sensitive to second-order nonlinearity as shown in Fig. 3. The algorithms from class B have a periodic phase error dependence as shown in Fig. 4. The P-V phase error plot in Fig. 3 represents maximum error changes (detector nonlinearity is expressed in percent). The phase error caused by second-order detector nonlinearity for class B methods exists; however, values are not significant for most detectors.

### C. Fourier Analysis of Sampling Functions

We can also examine the sensitivity of algorithms to phase-shift miscalibration and detector nonlinearity by looking at the spectrum of the sampling function.<sup>8,16</sup> However, to analyze algorithms in this way we find it convenient to express the incoming and reference signals in different mathematical forms. The incoming intensity signal at a given pixel can be written as

$$I(t) = I[1 + \gamma \cos(2\pi\nu t + \phi)], \quad (14)$$

where  $\nu$  is the modulation frequency and  $t$  is a temporal phase-shift parameter. In the synchronous detection process the incoming signal is correlated with the reference signal [Eq.(1)]. The reference signals of frequency  $\nu_f$  and phase-shift parameter

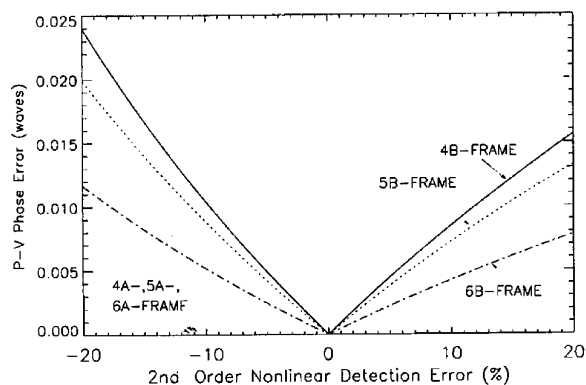


Fig. 3. P-V phase error versus percent of second-order detector nonlinearity error.

$t$  can be written in the form of functions:

$$\begin{aligned} f_N(t) &= -\sin(2\pi\nu_f t), \\ f_D(t) &= \cos(2\pi\nu_f t). \end{aligned} \quad (15a)$$

Ideally we want the frequencies of the measured and reference signals to be equal ( $\nu = \nu_f$ ). If this is not the case then we have phase-shift miscalibration.

For the conventional phase-stepping process, functions  $f_N(t)$  and  $f_D(t)$  are the equispaced samples of sine and cosine functions, respectively [Eq. (1)] and can be called sampling functions. Generally these samples can have additional weighting coefficients, and the sampling functions can be written as

$$\begin{aligned} f_N(t) &= -\sum_{m=1}^M \alpha_m \sin(2\pi\nu_f t) \delta(t - t_m), \\ f_D(t) &= \sum_{m=1}^M \beta_m \cos(2\pi\nu_f t) \delta(t - t_m), \end{aligned} \quad (15b)$$

where  $\alpha_m, \beta_m$  are the weighting coefficients of the  $m$ th

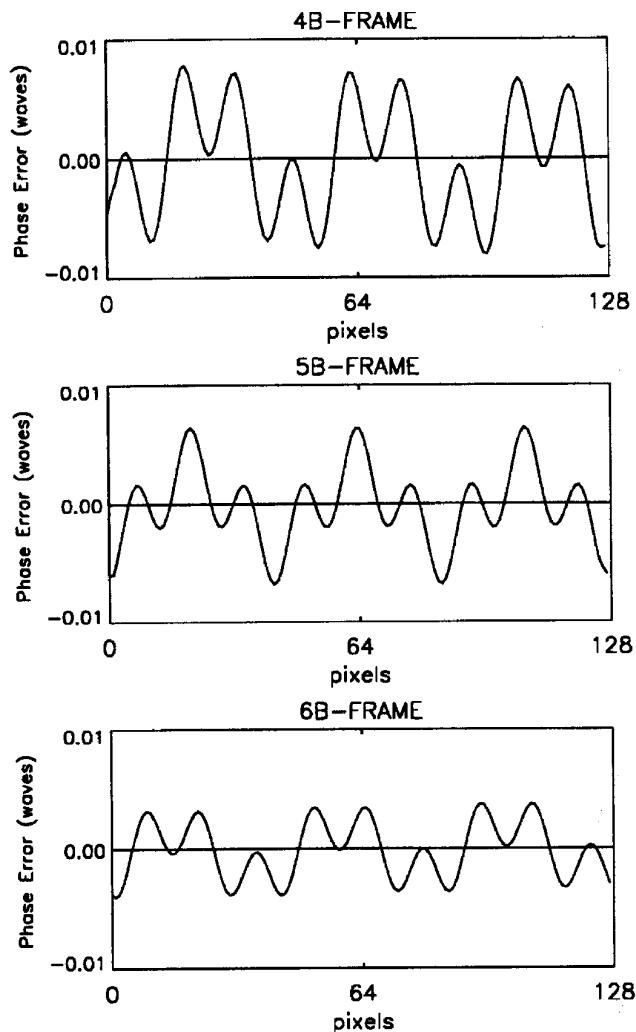


Fig. 4. Phase error for three intensity fringes caused by 10% second-order detector nonlinearity error.

discrete sample,  $\delta$  is a delta function, and  $t_m$  gives the sample position. For the chosen forms of the 4- and 5-frame methods presented here, the sampling functions in the numerator and denominator are as follows. For the 4A-frame algorithm, we have

$$\begin{aligned} f_N(t) &= -\delta\left(t - \frac{\pi}{4}\right) - \delta\left(t - \frac{3\pi}{4}\right) + \delta\left(t - \frac{5\pi}{4}\right) - \delta\left(t - \frac{7\pi}{4}\right), \\ f_D(t) &= \delta\left(t - \frac{\pi}{4}\right) - \delta\left(t - \frac{3\pi}{4}\right) - \delta\left(t - \frac{5\pi}{4}\right) + \delta\left(t - \frac{7\pi}{4}\right). \end{aligned} \quad (16a)$$

For the 5A-frame algorithm, we have

$$\begin{aligned} f_N(t) &= -\delta\left(t - \frac{\pi}{2}\right) + \delta\left(t - \frac{3\pi}{2}\right), \\ f_D(t) &= \delta(t)/2 - \delta(t - \pi) + \delta(t - 2\pi)/2. \end{aligned} \quad (16b)$$

For the 4B-frame algorithm, we have

$$\begin{aligned} f_N(t) &= -\delta\left(t - \frac{3\pi}{8}\right) + \delta\left(t - \frac{5\pi}{8}\right), \\ f_D(t) &= \frac{1}{2}\left[\delta\left(t - \frac{\pi}{4}\right) - \delta\left(t - \frac{3\pi}{4}\right) - \delta\left(t - \frac{5\pi}{4}\right) + \delta\left(t - \frac{7\pi}{4}\right)\right]. \end{aligned} \quad (16c)$$

For the 5B-frame algorithm, we have

$$\begin{aligned} f_N(t) &= \frac{1}{6}\left[\delta(t) - 4\delta\left(t - \frac{\pi}{2}\right) + 4\delta\left(t - \frac{3\pi}{2}\right) - \delta(t - 2\pi)\right], \\ f_D(t) &= \frac{1}{6}\left[\delta(t) + 2\delta\left(t - \frac{\pi}{2}\right) - 6\delta(t - \pi) + 2\delta\left(t - \frac{3\pi}{2}\right) + \delta(t - 2\pi)\right]. \end{aligned} \quad (16d)$$

Equations (16a)–(16d) have been normalized so that the maximum value equals unity. The graphic representations for chosen forms of all the methods are presented in Fig. 5.

As the number of frames increases, the weighting coefficients have their maximum value at the central sample and the values of the coefficients gradually fall off for the surrounding samples. The importance of weighting coefficients has been discussed in a few papers,<sup>8,16,17</sup> but the values of the weighting coefficients have never been explicitly given. We obtained the set of weighting coefficients fairly easily for the new 5- and 6-frame methods, which significantly reduced the errors of the methods. The weighting of data technique is often used in the Fourier transform phase measurement<sup>18</sup> to reduce the phase error.

To discuss the performance of algorithms we need to look at the frequency spectra of the above sampling functions, which are given here. For the 4A-frame

algorithm, we have

$$\begin{aligned} F_N(v) &= -2i \sin\left(\frac{\pi}{4} \frac{v}{v_f}\right) - 2i \sin\left(\frac{3\pi}{4} \frac{v}{v_f}\right) \exp\left(-i \frac{3\pi}{4} \frac{v}{v_f}\right), \\ F_D(v) &= -2 \cos\left(\frac{\pi}{4} \frac{v}{v_f}\right) + 2 \cos\left(\frac{3\pi}{4} \frac{v}{v_f}\right) \exp\left(-i \frac{3\pi}{4} \frac{v}{v_f}\right). \end{aligned} \quad (17a)$$

For the 5A-frame algorithm, we have

$$\begin{aligned} F_N(v) &= -2i \sin\left(\frac{\pi}{2} \frac{v}{v_f}\right) \exp\left(-i\pi \frac{v}{v_f}\right), \\ F_D(v) &= \left[-1 + \cos\left(\pi \frac{v}{v_f}\right)\right] \exp\left(-i\pi \frac{v}{v_f}\right). \end{aligned} \quad (17b)$$

For the 4B-frame algorithm, we have

$$\begin{aligned} F_N(v) &= -2i \sin\left(\frac{\pi}{4} \frac{v}{v_f}\right) \exp\left(-i \frac{3\pi}{4} \frac{v}{v_f}\right), \\ F_D(v) &= \left[\cos\left(\frac{3\pi}{4} \frac{v}{v_f}\right) + \cos\left(\frac{\pi}{4} \frac{v}{v_f}\right)\right] \exp\left(-i \frac{3\pi}{4} \frac{v}{v_f}\right). \end{aligned} \quad (17c)$$

For the 5B-frame algorithm, we have

$$\begin{aligned} F_N(v) &= -\frac{1}{3}i \left[4 \sin\left(\frac{\pi}{2} \frac{v}{v_f}\right) - \sin\left(\pi - \frac{v}{v_f}\right)\right] \exp\left(-i\pi \frac{v}{v_f}\right), \\ F_D(v) &= \frac{1}{3} \left[-6 + 4 \cos\left(\frac{\pi}{2} \frac{v}{v_f}\right) + 2 \cos\left(\pi \frac{v}{v_f}\right)\right] \exp\left(-i\pi \frac{v}{v_f}\right). \end{aligned} \quad (17d)$$

We focus on both the first and second harmonics of the spectrum, the first because it contains information about the tolerance to the phase-shift miscalibration, and the second because it represents the algorithm's sensitivity to second-order detector nonlinearity. At the first harmonic (normalized frequency equals 1) and nearby frequencies we are interested in the gradients of the spectra functions. Gradients of  $F_N$  and  $F_D$  at the first harmonic describe the algorithm's sensitivity to phase-shift miscalibration. Figure 6 shows a graphic representation of amplitudes of  $F_N$  and  $F_D$  for sampling functions from Fig. 5. For the 4A-frame algorithm the gradients at the first harmonic have different signs, resulting in high phase error. For both classes as the number of grabbed frames increases, the gradients around the first harmonic come into better alignment, reducing the error caused by phase-shift miscalibration. At the second-order harmonic we are interested in values of both spectra. If both spectra  $F_N$  and  $F_D$  have a zero value at the same time at the second harmonic (normalized frequency equals 2), then the algorithm is insensitive to second-order nonlinearity, provided there is no phase-shift miscalibration, or any other measurement nonlinearity that results in the second

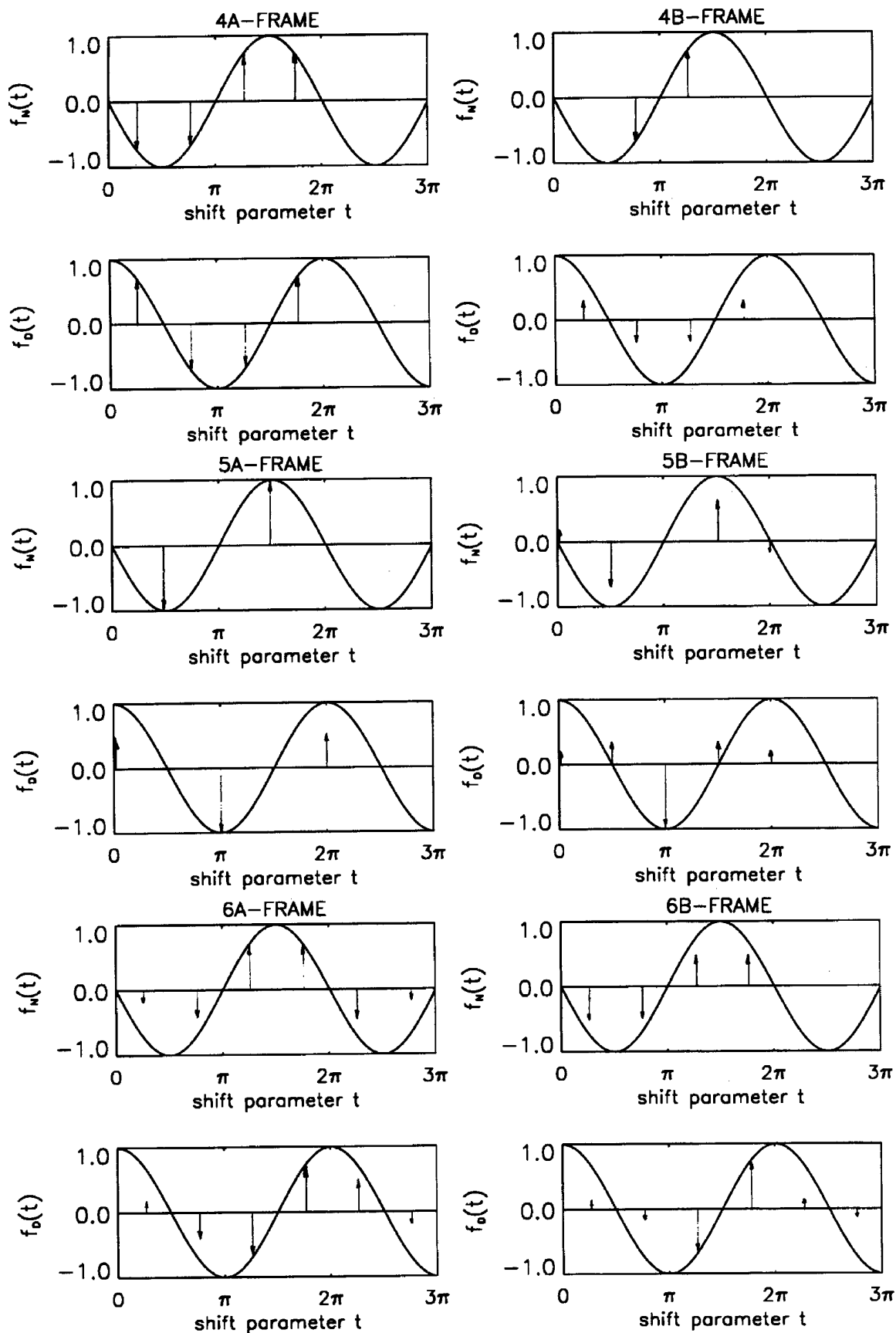


Fig. 5. Sampling functions.

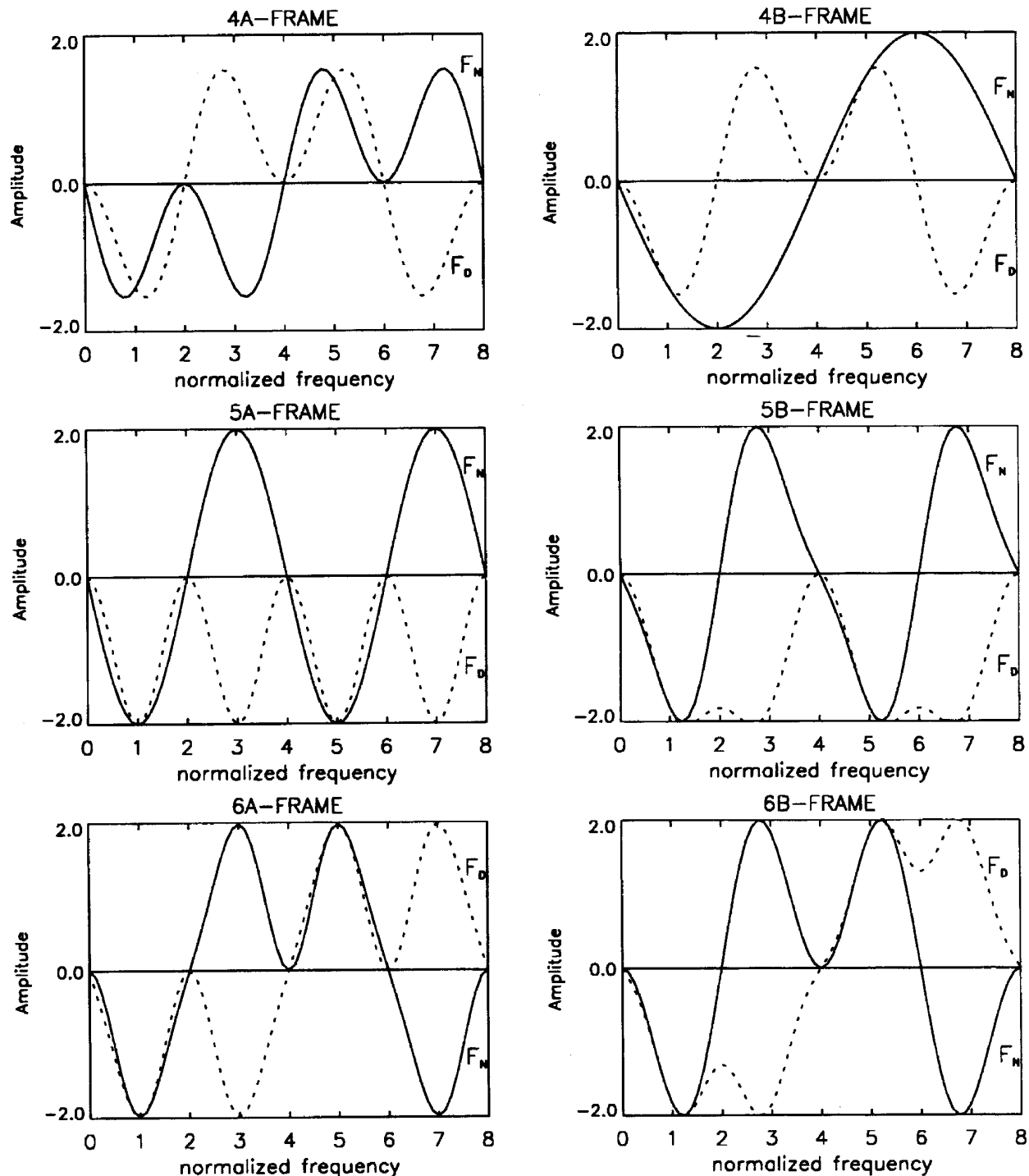


Fig. 6. Frequency spectra of sampling functions.

harmonic in the fringe pattern. All the algorithms from class A show such insensitivity. Algorithms from class B are sensitive to second-order detector nonlinearity, but this sensitivity decreases with the increasing number of frames taken.

## 5. Summary

We have presented an extended averaging technique based on the averaging technique introduced by Schwider. This technique permits the derivation of

many error-compensating algorithms in phase-shifting interferometry, if the averaging technique is applied sequentially. Fairly simple algorithms can be calculated if the phase shift between frames equals  $\pi/2$ . We derived two classes of algorithms for up to six frames of data, the first based on the common 3-frame algorithm (class A) and the second based on the 4-frame algorithm (class B). The 5A-frame and the 6A- and 6B-frame error-compensating algorithms were presented for the first time (to our knowledge) in

the literature. We analyzed the sensitivity of the four-, five-, and six-frame algorithms to phase-shift miscalibration and detector nonlinearity. The five- and six-frame methods were shown to be more tolerant to phase-shift miscalibration than any other method considered. The algorithms from class A are not sensitive to second-order detector nonlinearity. The algorithms from class B show some sensitivity to second-order detector nonlinearity, but the values of the error are rather insignificant for most detectors. The phase error caused by phase-shift miscalibration is smaller for algorithms from class B than for those from class A with the same number of frames. We can further develop in sequence algorithms that yield smaller and smaller phase errors. However, because the fast analysis of data is a priority, a small number of grabbed frames is more practical. The 6A-frame method combines the advantage of high tolerance for phase-shift miscalibration with a reasonably short process time and no sensitivity to second-order detector nonlinearity.

## References

1. J. Schwider, "Advanced evaluation techniques in interferometry," in *Progress in Optics*, E. Wolf, ed. (Elsevier, New York, 1990), Vol. 28, Chap. 4, pp. 271–359.
2. K. Creath, "Phase measurement interferometry techniques," in *Progress in Optics*, E. Wolf, ed. (Elsevier, New York, 1988), Vol. 26, Chap. 5, pp. 349–383.
3. J. H. Bruning, D. H. Herriott, J. E. Gallagher, D. P. Rosenfeld, A. D. White, and D. J. Brangaccio, "Digital wavefront measuring interferometer for testing optical surfaces and lenses," *Appl. Opt.* **13**, 2693–2703, (1974).
4. J. C. Wyant, "Interferometric optical metrology: basic system and principles," *Laser Focus* 65–71 (1982).
5. J. C. Wyant, C. K. Koliopoulos, B. Bhushan, and O. E. George, "An optical profilometer for surface characterization of magnetic media," *ASLE Trans.* **27**, 101–113 (1984).
6. J. E. Grievenkamp, "Generalized data reduction for heterodyne interferometry," *Opt. Eng.* **23**, 350–352 (1984).
7. C. J. Morgan, "Least-squares estimation in phase-measurement interferometry," *Opt. Lett.* **7**, 368–373 (1982).
8. K. G. Larkin and B. F. Oreb, "Design and assessment of symmetrical phase-shifting algorithms," *J. Opt. Soc. Am. A* **9**, 1740–1748 (1992).
9. Y. Surrel, "Phase stepping: a new self-calibrating algorithm," *Appl. Opt.* **32**, 3598–3600 (1993).
10. P. Hariharan, B. F. Oreb, and T. Eiju, "Digital phase-shifting interferometry: a simple error-compensating phase calculation algorithm," *Appl. Opt.* **26**, 2504–2505 (1987).
11. J. Schwider, R. Burow, K. E. Elssner, J. Grzanna, R. Spolaczyk, and K. Merkel, "Digital wave-front measuring interferometry: some systematic error sources," *Appl. Opt.* **22**, 3421–3432 (1983).
12. J. Schwider, O. Falkenstorfer, H. Schreiber, A. Zoller, N. Streibl, "New compensating four-phase algorithm for phase-shift interferometry," *Opt. Eng.* **32**, 1883–1885 (1993).
13. J. C. Wyant and K. N. Prettyjohns, "Optical profiler using improved phase shifting interferometry," U.S. patent 4,639,139 (27 January 1987).
14. K. Creath, "Temporal phase measurement methods," in *Interferogram Analysis: Digital Fringe Pattern Measurement Technique*, D. W. Robinson and G. T. Reid, eds. (Institute of Physics Publishing, Philadelphia, 1993), Chap. 4, pp. 94–140.
15. K. Creath and P. Hariharan, "Phase shifting errors in interferometric tests with high-numerical-aperture reference surfaces," *Appl. Opt.* **33**, 24–26 (1994).
16. K. Freischald and C. Koliopoulos, "Fourier description of digital phase-measuring interferometry," *J. Opt. Soc. Am. A* **7**, 542–551 (1990).
17. K. H. Womack, "Interferometric phase measurement using spatial synchronous detection," *Opt. Eng.* **23**, 391–395 (1984).
18. M. Kujawinska and J. Wojciak, "High accuracy Fourier transform fringe pattern analysis," *Opt. Lasers Eng.* **14**, 325–339 (1991).